Whole-Ecosystem Climate Manipulation Effects on Total Mercury within a Boreal Peatland

Caroline Pierce (pierc521@umn.edu)
University of Minnesota Twin Cities: University of Minnesota Twin Cities https://orcid.org/0000-0002-1930-5985

Sona Psarska
Minnesota Pollution Control Agency

Brandy D. Stewart
University of Minnesota Twin Cities: University of Minnesota Twin Cities

Keith C. Oleheiser
Oak Ridge National Laboratory

Natalie A. Griffiths
Oak Ridge National Laboratory

Jessica L. M. Gutknecht
University of Minnesota Twin Cities: University of Minnesota Twin Cities

Randall K. Kolka
US Forest Service: US Department of Agriculture Forest Service

Stephen D. Sebestyen
US Forest Service: US Department of Agriculture Forest Service

Edward A. Nater
University of Minnesota Twin Cities: University of Minnesota Twin Cities

Brandy M. Toner
University of Minnesota Twin Cities: University of Minnesota Twin Cities

Research Article

Keywords:

Posted Date: April 28th, 2023

DOI: https://doi.org/10.21203/rs.3.rs-2207553/v2

Whole-Ecosystem Climate Manipulation Effects on Total Mercury within a Boreal Peatland

Caroline E. Pierce [a], Sona Psarska [a b], Brandy D. Stewart [a], Keith C. Oleheiser [c d], Natalie A. Griffiths [c], Jessica L. M. Gutknecht [a], Randall K. Kolka [d], Stephen D. Sebestyen [d], Edward A. Nater [a], Brandy M. Toner [a]

a Department of Soil, Water, and Climate, University of Minnesota, St. Paul, MN 55108

b Current Affiliation: Minnesota Pollution Control Agency, Saint Paul, MN, 55155

c Environmental Sciences Division, Oak Ridge National Laboratory, Oak Ridge, TN 37831

d USDA Forest Service, Northern Research Station, Grand Rapids, MN 55744

Corresponding author email: toner@umn.edu

KEY WORDS: mercury, peat, climate change, temperature, carbon dioxide, water table

ABSTRACT

Mercury is a ubiquitous pollutant that accumulates in peatlands, an ecosystem highly sensitive to climate change. We examined the effects of increasing temperature and elevated atmospheric carbon dioxide (CO_2) on the concentration of total mercury (THg) in peatland soil and porewater. This research was performed at the Spruce and Peatland Responses Under Changing Environments (SPRUCE) experiment, an ecosystem-scale manipulation in an ombrotrophic bog in northern Minnesota, USA, which includes five temperature levels (above- and below-ground warming), with ambient or enhanced CO_2 concentration. Increasing temperature led to increased $THg_{porewater}$ concentrations and these increases were correlated with physical (water table height) and chemical (pH, dissolved sulfate, total dissolved iron, solid-state sulfur speciation) environmental factors. The ratio of THg_{peat} to $THg_{porewater}$ decreased with warming, indicating that THg moved from the peat into porewater. In the top portion of the depth profile (0 cm to -40 cm), a net movement of THg from peat to porewater was observed with elevated CO_2. This finding is likely due to indirect effects of elevated CO_2 such as the lowering of the water table and changes in the

proportion of plant species. Porewaters had more detectable changes in THg than peat. Peat with higher proportions of organic disulfide were observed to retain more THg in the solid phase than peat with higher proportions of organic monosulfide (thiols). Overall, we observed that temperature and CO_2 had significant but subtle effects on THg in porewater. Our findings indicate with projected climate change, we may see some enhanced concentrations of THg available for export to surface waters. However, the first three years of temperature and CO_2 treatments suggest that this could be a relatively small change to local surface water loadings.

1. INTRODUCTION

Mercury (Hg) is a persistent, global, atmospheric pollutant. Emissions of mercury arise from anthropogenic sources such as coal burning, mining, and industrial activities. These human activities have increased the amount of atmospheric mercury globally by 450 % to 660 % (Lindberg et al. 2007; Amos et al. 2013; Zhang et al. 2014; Outridge et al. 2018). Inorganic mercury, in both gaseous and particulate forms, is emitted as an atmospheric pollutant (Lindberg et al. 2007; Driscoll et al. 2013; Li et al. 2020). Depending on the form of mercury, it can be deposited locally, regionally, or travel long distances from point sources before being deposited into terrestrial systems including peatlands (Grigal 2003; Lindberg et al. 2007; Driscoll et al. 2013; Li et al. 2020). The accumulation rate of mercury in peat bogs increased by a factor of ~26 between the pre-anthropogenic period and the 20th century peak (Outridge et al. 2018). Peatlands contain large amounts of carbon and are a mercury sink because of the strong affinity between mercury and organic matter (Meili 1991). In particular, Hg(II) binds to reduced sulfur species found in organic matter (Skyllberg 2008; Nagy et al. 2011).

In peatlands, total mercury (THg) refers to the sum of all mercury species present: elemental mercury, inorganic mercury, methylmercury (MeHg), among other organic mercury species. The mercury species of most concern is MeHg due to its toxicity at environmentally relevant levels and ability to bioaccumulate and biomagnify in the food web (Inskip et al. 1985; Clarkson and Magos 2006; Selin 2009; Driscoll et al. 2013). Methylmercury comprises generally less than 5% of THg in ombrotrophic peat and is highly variable (0.2% to 60%) in porewater in peatlands (Grigal 2003; Skyllberg et al. 2003; Mitchell et al. 2008a; Coleman Wasik et al. 2012; Haynes et al. 2017a; Hu et al. 2020; Wang et al. 2020, 2021). Peatlands are sources of MeHg to surface waters through the direct release of MeHg (Benoit et al. 2003; Selin 2009; Xu et al. 2021) and the indirect release of mercury that is later transformed into MeHg downstream. Mercury leaves the peatland system through surface and subsurface lateral flow, also called outflow (Verry et al. 2011b; Sebestyen and Griffiths 2016). In aquatic systems, MeHg biomagnifies in the food web to top

predatory fish which can then be consumed by wildlife and humans, ultimately resulting in health effects (Ullrich et al. 2001). It has been shown that wetland area within a watershed is directly correlated to mercury concentration in fish (Simonin et al. 2008; Gabriel et al. 2009; Driscoll et al. 2013; Osgood et al. 2022). Another route of mercury emission is gaseous mercury evasion to the atmosphere (Haynes et al. 2017b; Osterwalder et al. 2017; O'Connor et al. 2019). The evasion of mercury from peat to the atmosphere is estimated to be seven-times higher than the loss of mercury through water (Osterwalder et al. 2017).

Boreal peatlands contain approximately 30 % of global terrestrial carbon and are important zones of element retention and biogeochemical cycling (Gorham 1991; Urban et al. 2011; Yu 2012). Projected climate change of the northern hemispheric boreal ecotone is likely to alter this biogeochemical cycling with consequences for environmental quality at local, regional, and global scales (Hilbert et al. 2000; Ise et al. 2008; Shi et al. 2015). Increases of 1 °C - 5.7 °C in global mean annual air temperature by the year 2100 are projected using global models with even larger increases at higher latitudes, where most peatlands are located (IPCC 2021). Warmer temperatures, longer frost-free periods, longer dry conditions in the summer, and more intense precipitation events are forecasted to occur along the southern boreal—northern deciduous forest ecotone (Ma et al. 2012; Yu et al. 2016). Overall, precipitation is expected to increase but it will be concentrated in more intense storms with longer and more frequent droughts in between (Yu et al. 2016; IPCC 2021). Additionally, with higher temperatures, evapotranspiration is anticipated to increase which will lead to a lowering of the water table in peatlands (Andersen et al. 2013; Shi et al. 2015). Research in Arctic permafrost peatlands have shown that increasing temperatures have already caused an increase in the release of inorganic mercury (Gordon et al. 2016). Boreal peatlands are projected to get drier and may therefore not respond in the same way as Arctic peatlands which have thawing permafrost leading to wetter conditions (Hanson et al. 2020). Previous studies in peatlands have measured the impact of climate change on the mobility and transport of mercury in porewaters by altering the water table and plant functional groups (Haynes et al. 2017a). The effects of temperature and CO_2 on the internal cycling and mobilization of THg to porewaters in peatlands have not yet been reported. To our knowledge, there are no known direct effects of atmospheric CO_2 on terrestrial mercury cycling. However, there may be indirect effects of increased atmospheric CO_2 on peatland mercury through changes in the productivity of plants and the height of the water table (Norby et al. 2010; De Kauwe et al. 2013; Reyer et al. 2014; Xu et al. 2016).

Our objective was to investigate the impact of warming and elevated CO_2 on THg concentration in peatland soil and porewater. We expected that increases in temperature would increase mercury release from peat to porewaters. The

Spruce and Peatland Responses Under Changing Environments (SPRUCE) experiment (described in section 2.2) is a unique, large-scale climate manipulation to study the impact of increasing temperature and elevated CO_2 on a boreal peatland. In this study, we measured the porewater concentrations of THg, total organic carbon (TOC), sulfate, total iron, and pH, as well as the peat concentrations of THg, percentages of carbon, nitrogen, and sulfur (by weight), and the speciation of sulfur in peat. Associated environmental variables that were measured were the water table height and soil temperature at multiple depths.

2. MATERIALS AND METHODS

2.1 Site Description

The research was conducted in the S1 bog, the site of the SPRUCE experiment, at the U.S. Department of Agriculture (USDA) Forest Service Northern Research Station, Marcell Experimental Forest (MEF, Figure S1, Sebestyen et al. 2021). The site is located 40 km north of Grand Rapids, MN, USA, at 47.50515406 degrees N; 93.45398586 degrees W. The S1 bog is an ombrotrophic peatland (i.e., a bog) dominated by trees: *Picea mariana* (black spruce) and *Larix laricina;* ericaceous shrubs: *Rhododendron groenlandicum, Chamaedaphne calyculata,* and *Vaccinium angustifolium;* a variety of sedges (*Carex* spp.); and *Sphagnum* spp. mosses (Hanson et al. 2017). The peatland soil is the Greenwood series, a Typic Haplohemist, with average peat depths of 2 m - 3 m (Parsekian et al. 2012). The climate of MEF is subhumid continental with strong diurnal and seasonal temperature fluctuations. The mean annual temperature from 1961 to 2019 was 3.5 ℃ with a minimum of -46 ℃ and a maximum of 38 ℃ (Sebestyen et al. 2021). Mean annual precipitation over the same period was 787 mm with $^2/_3$ occurring during the snow-free period (Sebestyen et al. 2011, 2021). From 1961 to 2009, average annual temperatures have increased about 0.4 °C each decade (Sebestyen et al. 2011).

Peatlands are permanently or semi-permanently saturated resulting in slow decomposition rates leading to an accumulation of organic matter. Bogs lack inputs from groundwater which results in an ombrotrophic system. All inputs are from atmospheric deposition (Bourbonniere 2009). The soil depth profile can be classified into two sections: the acrotelm and catotelm. The acrotelm is the top layer and characterized by low density, comparatively high hydraulic conductivity, transiently oxic conditions depending on water table fluctuations, and includes living plants and the majority of roots (Nungesser 2003). The catotelm, below the acrotelm, is permanently saturated (during non-drought years) and tends to have higher density and lower hydraulic conductivity (Verry et al. 2011a; Tfaily et al. 2014).

2.2 Description of the SPRUCE Experiment

At SPRUCE, there are 10 open-topped enclosures, each with a different temperature and CO_2 level (Figure S2). The experimental temperature levels in air and soil with respect to ambient temperature are +0 °C (control), +2.25 °C, +4.5 °C, +6.75 °C, and +9 °C and are maintained year-round (Hanson et al. 2017). Each temperature level has two enclosures: one at ambient atmospheric CO_2 and another with elevated atmospheric CO_2 concentrations (+500 ppm) during the growing season (approximately early April through early November). The various warming levels are maintained via above-ground and below-ground heating (except for the +0 °control ,Hanson et al. 2017). Treatments were not initiated simultaneously (Table 1). Each open-topped enclosure is 7.0 m tall by 12.8 m diameter, with a 35° frustum, and a surface area of 114.8 m^2 (Hanson et al. 2017). Each enclosure is surrounded underground by a corral composed of interlocking vinyl sheet-pile walls that extend to the glacial till to hydrologically isolate the enclosure from the surrounding bog (Sebestyen and Griffiths 2016; Hanson et al. 2017). Lateral outflow pipes were installed in the near-surface peat of each enclosure, which allow for passive water drainage and water table fluctuations (Sebestyen and Griffiths 2016). The above-ground walls of the enclosure are composed of structural aluminum and double-walled transparent greenhouse panels (Hanson et al. 2017).

Table 1 *Timeline of treatment initiation at the SPRUCE site. (Hanson et al. 2017)*

Activity Description	Date
Soil temperature treatment initiated	July 2, 2014
Air temperature treatment initiated	August 13, 2015
Carbon dioxide treatment initiated	June 15, 2016

2.3 Sampling Method

Between 2017 and 2019, porewater was collected every two weeks, during the non-frozen period (typically April/May to October/November) from a nest of four piezometers in each enclosure (depths of openings: 0 cm to -10 cm, -30 cm to -40 cm, -50 cm to -60 cm, and -100 cm to -110 cm, a depth of 0 cm is equivalent to the peat surface). The piezometers, made of polyvinyl chloride (PVC), were evacuated several hours before each sampling event to obtain fresh porewater. An unfiltered water sample was pumped from each piezometer using a peristaltic pump connected with a silicone sampling tube. Sample water was pumped into a clean 125 mL polyethylene terephthalate glycol (PETG) bottle that was rinsed 3 times with sample water before being filled. The 125 mL sample was preserved with 0.5 mL trace metal hydrochloric acid and refrigerated before shipping to the lab for analysis.

Once a year between 2017 and 2019, in mid-August, a peat core was collected from each enclosure. The peat cores were composed of 11 depth increments to a depth of -200 cm resulting in a total of 110 samples per year. A 7.5 cm stainless steel drill (rotary) corer was used to collect surface samples (0 cm to -30 cm, Iversen et al. 2014) and deeper peat cores were collected with a Russian peat corer (Jowsey 1966). Depths 0 cm to -50 cm were divided in 10 cm increments and depths -50 cm to -200 cm were divided in 25 cm increments (Iversen et al. 2014). Subsamples for sulfur speciation were placed in 40 mL IChem glass vials (SB360040, Thermo Scientific, Rockwood TN, USA), purged of ambient atmosphere, and the headspace was replaced with argon in the field. The samples were then placed in mylar pouches containing Anaeropack oxygen scrubbers (R681001, Mitsubishi Gas Chemical Co., Tokyo, Japan) and stored in a freezer. All samples for sulfur analyses were protected from ambient atmosphere during sample shipping, storage, and analysis (Pierce et al. 2022). Subsamples for mercury analyses were placed in 40 mL polypropylene specimen cups and stored frozen until freeze-dried for further analysis.

2.4 Mercury Sample Preparation and Analysis

Prior to THg analysis, freeze-dried peat samples were digested in concentrated nitric acid overnight at 70 ºC (Bloom and Crecelius 1983; Grigal et al. 2000).

Porewater samples were not filtered prior to analysis because no filtration (TOC) and 0.7 μm filtration (dissolved organic carbon, DOC) provide equivalent measures of organic carbon concentration at our field site and TOC had strong explanatory power for THg in water (Sebestyen et al. 2011, 2020, 2021). For porewater samples, at least 25 mL of sample was transferred into a 125 mL Teflon bottle and 2 - 4 mL (1:1000 based on darkness of sample) of bromine monochloride (BrCl) was added to digest the sample. The samples were placed in a 70 °C oven and digested overnight. After digestion, the remaining BrCl in the sample was reduced by pipetting 0.4 - 0.8 mL of hydroxylamine hydrochloride into the solution and mixed.

Peat and porewater samples were analyzed following U.S. Environmental Protection Agency (EPA) Method 1631 for determination of THg by oxidation, purge, double gold amalgamation trap, desorption, and cold-vapor atomic fluorescence spectrometry (CVAFS, U.S. Environmental Protection Agency 2002) on a Tekran Series 2600-IVS analyzer. The method was modified by using unfiltered water samples.

Each digested and reduced sample was transferred to a 40 mL IChem glass vial. A quantity of 60 μL of stannous chloride ($SnCl_2$) was added, and the vial was immediately capped. The sample was allowed to react for 30 minutes, prior to analysis, to allow time for the $SnCl_2$ to convert the Hg(II) to gaseous Hg(0).

For quality assurance / quality control, ten percent of samples were analyzed in duplicate or spiked with known amounts of mercury (Table S1). In addition, blanks and check standards were run approximately every 15 samples. The detection limit was 0.03 ng g^{-1} for peat and 0.2 ng L^{-1} for porewaters.

2.5 Sulfur Speciation in Peatland Soil

Sample handling, processing, and storage followed published methods (Pierce et al. 2022). Briefly, peat samples were dried in a Bel-art gas purge box (F42072-1009, Wayne NJ, USA) and flushed with nitrogen continuously for 7 - 8 days at room temperature. Dried peat was homogenized under liquid nitrogen using a ceramic mortar and pestle in a glovebag, split for multiple analyses, and sealed in nitrogen-filled mylar pouches before further analyses.

Sulfur 1s X-ray absorption near edge structure (XANES) spectroscopy was used to acquire sulfur speciation data using established and nondestructive methods (Manceau and Nagy 2012; Zeng et al. 2013; Cron et al. 2020; Pierce et al. 2022). The data were acquired on the 06B1-1 Soft X-ray Microcharacterization Beamline (SXRMB) at the Canadian Light Source (CLS, Saskatoon, SK, Canada). At the CLS beamline, ground samples were applied on a low-sulfur double-adhesive carbon tape and attached to a copper multi-sample plate in ambient air. Samples were exposed to oxygen for 30 - 45 minutes. Sample splits prepared in a glove bag and on the benchtop have demonstrated no change in the oxidative state of the sulfur for this duration of exposure (see supplemental text, "Assessment of XANES Glovebag Preparation vs. Ambient Benchtop Preparation"). The prepared holders were sealed in a mylar bag with argon until placed into the sample chamber under a vacuum for analysis by simultaneous total electron yield (TEY) and fluorescence detection. Photon damage to the samples was not observed and each spectrum was the average of two to three scans per sample. Energy calibration of the monochromator was performed using gypsum ($CaSO_4$) with the absorption maximum set to a value of 2482.74 eV (Cron et al. 2020; Pierce et al. 2022).

Sulfur XANES spectra were energy calibrated, averaged, pre-edge subtracted, and post-edge normalized in *Athena* (Ravel and Newville 2005). Linear combination fitting (LCF) of the sample spectra with reference spectra was performed using *mrfitty* (Nicholas et al. 2017) applying the published sulfur reference database in Pierce et al. (2022). See the Supplemental Information for "Assessment of Error in Linear Combination Fitting". The fitting of a reference, for example: L-cystine (organic disulfide, R-S-S-R'), does not indicate that L-cystine is in the sample. It indicates that the sulfur in the sample has a bonding and valance state similar to the sulfur in the reference material. Therefore, LCF results are binned to translate from specific reference spectra (e.g., L-cystine) to the sulfur species it represents (e.g., organic disulfide). See Table S2 for a description of each sulfur reference compound and binning group.

194 **2.6 Peat Percent Total Carbon, Nitrogen, and Sulfur**

195 Dried and ground samples were analyzed through combustion analysis of bulk peat samples (15.000 mg ± 0.005 mg)
196 using an Elementar Pyrocube combustion analyzer (varioPYRO cube, Elementar Inc, New Jersey, US). Certified
197 standard material acetanilide (Elemental Microanalysis, item: B2114) was used for carbon (71.09%) and nitrogen
198 (10.36%) and certified standard material sulfanilamide was used for sulfur (18.62%, Elementar, item: 15.00-0062).
199 Correction values were calculated to adjust the measurement of the certified standard materials to the accurate
200 elemental values. These correction values were then applied to the experimental samples. The detection limit was
201 <0.1%.

202 **2.7 Porewater Chemical Analysis**

203 Porewater samples were analyzed at the USDA Forest Service Northern Research Station (Griffiths and Sebestyen
204 2016a).Total organic carbon (TOC) was selected as an independent variable because of the affinity between carbon
205 and mercury (Meili 1991). Total organic carbon was measured by Standard Method 5310B on a Shimadzu (Columbia
206 MD, USA) TOC-L (APHA 2017). Total organic carbon is essentially equivalent to DOC in this ecosystem due to
207 organic particles being less than 0.7 µm in diameter (Sebestyen et al. 2020). The independent variable pH was selected
208 because mercury desorption from soil has been observed with increasing pH (Yang et al. 2007; O'Connor et al. 2019).
209 pH was measured by Standard Method 4500-H+ B on a Mettler Toledo (Columbus OH, USA) DL53 Auto Titrator
210 (APHA 2017). Sulfate was selected as a variable because MeHg is produced as a byproduct of sulfate-reducing
211 bacteria (Benoit et al. 2003; Mitchell et al. 2008b). Sulfate and chloride were measured by Standard Method 4110-C
212 on a Thermo Scientific Dionex (Sunnyvale CA, USA) ICS-2100 (ion chromatography with suppressed conductivity
213 detection, APHA 2017). The detection limits are 0.3 mg sulfate L^{-1} and 0.2 mg chlorine L^{-1}. Chloride is a
214 geochemically conservative species in peat and was measured to support the assessment of evaporative concentration
215 (Bottrell and Novak 1997). Iron was selected as a variable because MeHg is produced as a byproduct of iron-reducing
216 bacteria (Benoit et al. 2003; Bravo et al. 2018). Total iron was measured by Standard method 3120 on a Thermo
217 Scientific (Waltham MA, USA) ICAP 7600 Duo with an ASX-520 Autosampler and Qtegra Intelligent Scientific Data
218 Solution Software (APHA 2017).

219 **2.8 Environmental Measurements**

220 A TruTrack (Christchurch, New Zealand) WTVO-2000 sensor placed in a stainless steel well in the center of each
221 enclosure was used to measure the water table height every 30 minutes (Hanson et al. 2020). Water table data were

expressed relative to the peat surface (0 cm) and are a daily average. Temperature probes were placed in the peat in triplicate (depths: 0 cm, -10 cm, -20 cm, -30 cm, -40 cm, -50 cm, -100 cm, and -200 cm) and temperature was recorded every 30 minutes (Hanson et al. 2020) resulting in 48 measurements per day at each depth per enclosure. The temperature measurements for each of the 8 depths were averaged per day and this is referred to throughout the manuscript as mean daily soil temperature. For porewater analyses, the temperature probes placed at depths 0 cm, -30 cm, -50 cm, and -100 cm were used.

2.9 Ratio of THg in Peat to THg in Porewater

The ratio of THg_{peat} to $THg_{porewater}$ (THg_{peat}:$THg_{porewater}$) is calculated as shown in equation 1.

$$[THg]_{peat} \Big/ [THg]_{porewater} \quad (1)$$

A caveat to this calculation is that peat and porewater were not sampled on the same day. The porewater sampling date closest to the once-a-year peat sampling was chosen for the calculation. The difference between the porewater sampling date and peat sampling date ranges from 3 to 5 days. We calculated the ratio of THg_{peat} to $THg_{porewater}$ by matching peat and porewater samples at 0-10 cm, and 30-40cm. At two other depths, we paired the closest depth increments. That is, 50-60 cm for porewater with 50-75 cm for peat, and 100-110 cm for porewater with 100-125 cm for peat. Ratios were not averaged.

2.10 Statistics

A regression-based approach was used to assess the results of this study. This method, as opposed to an ANOVA-based approach, generally offers more power and supports treatment levels without replication to describe the response of variables to elevated temperature and CO_2 (Cottingham et al. 2005). The regression-based approach has been used to examine the responses of other variables in SPRUCE (Norby et al. 2019; Hanson et al. 2020; McPartland et al. 2020; Wilson et al. 2021b; Curtinrich et al. 2022; Iversen et al. 2022).

Statistical analyses were performed in *R* 4.2.0 (R Core Team 2017) using base R and package 'agricolae' (v1.3.5; function: LSD.test, de Mendiburu and Yaseen 2020), package 'car' (v3.0.13; functions: Anova and vif, Fox and Weisberg 2019), and package 'emmeans' (v1.7.5; function: lstrends, Lenth 2022). When log-transformed, the THg data met assumptions of normality based on visual assessments of histograms and quantile-quantile plots. The water table data and THg_{peat}:$THg_{porewater}$ data did not meet assumptions of normality based on visual assessment but the water table data had a large sample size (n = 6,194) and by the central limit theorem, large samples sizes ($n \geq 50$) are well-approximated by a normal distribution even if the data themselves are not normally distributed (Stevens 2013). The

250 THg_{peat} to $THg_{porewater}$ ratio data did not have a large sample size (n = 30) and, therefore, were excluded from analyses
251 requiring a normal distribution. The response of THg_{peat}:$THg_{porewater}$ was assessed by using Spearman's rank
252 correlation for non-linear and non-parametric data with a significance level of $p < 0.05$. The relationship between
253 THg_{peat}:$THg_{porewater}$ and CO_2 level could not be assessed using Spearman's correlation as CO_2 treatment was a
254 categorical variable and not continuous.
255 To examine the treatment effects on THg concentrations in both peat and porewater, we used analysis of covariance
256 (ANCOVA), with CO_2 level as the factor, mean daily soil temperature (averaged across depths) as the covariate, THg
257 concentration (averaged across depths) as the dependent variable, and a significance level of $p < 0.05$. When analyzing
258 the full depth profile, the ANCOVA had a blocking factor of depth zone (acrotelm and catotelm, described in section
259 2.1). Mean THg concentration values across depths at each sampling timepoint were used in these ANCOVAs to
260 reduce pseudoreplication. An ANCOVA was also used to examine effects of mean daily soil temperature and CO_2
261 level on the daily water table height during the growing season. Pseudoreplication was reduced but not eliminated by
262 averaging the water table data per day. Multiple comparisons were performed using pairwise t-tests and p-values were
263 adjusted using Holm's correction method for multiple comparisons (Holm 1979).
264 Stepwise multiple linear regression (MLR) was used to evaluate the effect of experimental treatments and
265 environmental conditions on THg concentration for the full depth profile, the acrotelm, and the catotelm. For peat, the
266 full depth profile was 0 cm to -200 cm, acrotelm was 0 cm to -40 cm, and catotelm was -50 cm to -200 cm. For
267 porewater, the full depth profile was 0 cm to -110 cm, acrotelm was 0 cm to -40 cm, and catotelm was -50 cm to -110
268 cm. The following factors were used to determine their influence on the mercury concentrations within the porewater
269 samples ($THg_{porewater}$): depth (D), CO_2 level, mean daily soil temperature measured at the sampling depth (T), mean
270 seasonal water table height (W), total organic carbon (TOC) concentration, pH, sulfate concentration (SO_4^{2-}), and total
271 iron concentration (Fe). Even though the SPRUCE treatments were defined as discrete levels of warming, the
272 temperature is expressed and analyzed as the actual temperature measured because this is a biological system with
273 seasonality trends in temperature. Mean daily soil temperature and mean seasonal water table height were selected
274 based on the rationale presented in Feng et al. (2020) who identified daily soil temperature maximum and seasonal
275 water table elevation as the best performing models for predicting annual methane fluxes. Our own assessments of
276 goodness of fit for simple linear regressions between THg concentration and the means of daily, weekly, monthly,
277 annual, and seasonal measurements of soil temperature and water table height supported the selection of mean daily

soil temperature and mean seasonal water table height. The regression equation that expresses these factors and how they may influence mercury concentration in porewater is as follows:

$$y = \beta_0 + \beta_1 D + \beta_2 CO_2 + \beta_3 T + \beta_4 W + \beta_5 TOC + \beta_6 pH + \beta_7 SO_4^{2-} + \beta_8 Fe \quad (2)$$

Where y is the response variable [log($THg_{porewater}$ concentration)], β_0 is the intercept, and $\beta_{1\text{-}8}$ are the regression coefficients. The best stepwise model was selected using R^2 values and Akaike's information criterion (AIC). All references to differences in the results section refer to statistically significant differences ($p < 0.05$). For the analysis of the acrotelm and catotelm, the variable "depth" was excluded from the MLR.

The following factors were used in the regression of mercury concentrations within the peat samples (THg_{peat}): depth (D), CO_2 level, mean daily soil temperature measured at the sampling depth (T), mean seasonal water table height (W), ratio of carbon to nitrogen (C:N), percent sulfur by weight (%S), percent of ester sulfate out of total sulfur (ES), sulfone/sulfonate (SS), sulfoxide (S), thiol/monosulfide/thiophene (TMT), and organic disulfide (OD). The regression equation that expresses these factors and how they may influence mercury concentration in peat are as follows:

$$y = \beta_0 + \beta_1 D + \beta_2 CO_2 + \beta_3 T + \beta_4 W + \beta_5 C{:}N + \beta_6 \%S + \beta_7 ES + \beta_8 SS + \beta_9 S + \beta_{10} TMT + \beta_{11} OD \quad (3)$$

The carbon to nitrogen ratio was used because it is an indicator of the level of decomposition (Post et al. 1985; Sanderman and Amundson 2003). Following the determination of a MLR, the model was checked for multicollinearity using the variance inflation factor.

3. RESULTS

3.1 Effect of Temperature on THg Concentration

The following subsections will cover the effects of warming on THg_{peat} concentration, $THg_{porewater}$ concentration, and THg_{peat}:$THg_{porewater}$.

3.1.1 THg_{peat} Concentration

The ANCOVA results demonstrated that log-transformed THg_{peat} concentration did not have a significant relationship with mean daily soil temperature (Table 2). The MLR of log-transformed THg_{peat} concentration in the full depth profile resulted in an R^2 value of 0.60 with a significant p-value (< 0.0001) but did not include temperature as an influential variable (Table 3). When performing the MLR for the acrotelm (0 cm to -40 cm) and catotelm (-50 cm to -200 cm) separately, the variable depth was removed and the R^2 values decreased (Table 3). Temperature was not an influential variable in the acrotelm but it was in the catotelm and had a positive coefficient with log-transformed THg.

Table 2 *ANCOVA results for log-transformed THg_{peat} concentration, log-transformed $THg_{porewater}$ concentration, and non-transformed water table height. The factor variable was CO_2 level and the covariate was mean daily soil temperature. The interaction of temperature and CO_2 level is indicated by "Temperature*CO_2" The top panel has the results for the full depth profile and the bottom two panels are subset into the acrotelm and catotelm depths. Zone refers to the acrotelm and catotelm and was assessed as a blocking factor. For peat, the full depth profile was 0 cm to -200 cm, acrotelm was 0 cm to -40 cm, catotelm was -50 cm to -200 cm. For porewater, the full depth profile was 0 cm to -110 cm, acrotelm was 0 cm to -40 cm, catotelm was -50 cm to -110 cm. A significant p-value was < 0.05. Porewater n = 430, peat n = 30, and water table height n = 6,154.*

Full Depth Profile			
	p-values		
	Peat LogTHg	Porewater LogTHg	Water Table Height
Mean daily soil temperature	0.94	0.09	<0.0001 *
CO_2 Treatment	0.84	0.07	<0.0001 *
Temperature*CO_2	0.96	0.13	<0.01 *
Zone	<0.0001 *	<0.0001 *	
Zone: Acrotelm			
	p-values		
	Peat LogTHg	Porewater LogTHg	
Mean daily soil temperature	0.72	<0.001 *	
CO_2 Treatment	0.62	0.04 *	
Temperature*CO_2	0.68	0.54	
Zone: Catotelm			
	p-values		
	Peat LogTHg	Porewater LogTHg	
Mean daily soil temperature	0.54	0.90	
CO_2 Treatment	0.64	<0.01 *	
Temperature*CO_2	0.64	0.24	

* $\alpha < 0.05$

315 ***Table 3*** *Stepwise multiple linear regression (MLR) coefficients for log-transformed THg concentration. For peat, the full depth profile was 0 cm to -200 cm,*
316 *acrotelm was 0 cm to -40 cm, catotelm was -50 cm to -200 cm. For porewater, the full depth profile was 0 cm to -110 cm, acrotelm was 0 cm to -40 cm, catotelm*
317 *was -50 cm to -110 cm. Coefficients (β_k) and model performance from stepwise MLR analysis (Eq. 3) for peat with independent variables being depth (D),*
318 *elevated CO_2 (eCO_2), mean daily soil temperature (T), mean seasonal water table height (W), ratio of carbon to nitrogen (C:N), percent sulfur (%S), percent of*
319 *ester sulfate out of total sulfur (ES), sulfone/sulfonate (SS), sulfoxide (S), thiol/monosulfide/thiophene (TMT), and organic disulfide (OD) and dependent variable*
320 *log-transformed total mercury concentration [log10(THg_{peat})]. Coefficients (β_k) and model performance from stepwise MLR analysis (Eq. 2) for porewater with*
321 *independent variables being depth (D), elevated CO_2 (eCO_2), mean daily soil temperature (T), mean seasonal water table height (W), total organic carbon*
322 *concentration (TOC), pH, sulfate concentration (SO_4), total iron concentration (Fe), and dependent variable log-transformed total mercury concentration*
323 *[log10($THg_{porewater}$)]. Negative coefficients are indicated in red and positive coefficients are indicated in black. All linear regressions had a p-value < 0.0001. An*
324 *entry of "N/A" means the variable was not included in the equation as its addition either lowered the R^2 value or did not lower the AIC value.*

	Peat Independent variables												Model Summary [&]		
Depth Zone		D	eCO_2	T	W	C:N	%S	ES	SS	S	TMT	OD	n	R^2	R^2-adj
	β_0	β_1	β_2	β_3	β_4	β_5	β_6	β_7	β_8	β_9	β_{10}	β_{11}			
Full Profile	0.869	0.002	-0.058	N/A	0.016	0.005	2.505	0.014	0.017	-0.006	N/A	0.006	234	0.61	0.60
Acrotelm	1.653		-0.070	N/A	0.014	N/A	1.263	N/A	0.007	-0.012	N/A	0.007	146	0.42	0.40
Catotelm	0.523		-0.069	0.017	0.020	0.007	1.578	0.018	0.026	N/A	N/A	N/A	88	0.52	0.48
	Porewater Independent variables												Model Summary [&]		
		D	eCO_2	T	W	TOC	pH	SO_4	Fe				n	R^2	R^2-adj
	β_0	β_1	β_2	β_3	β_4	β_5	β_6	β_7	β_8						
Full Profile	1.603	0.007	N/A	0.003	-0.002	N/A	-0.189	0.223	0.029				1533	0.65	0.64
Acrotelm	1.558		0.093	0.007	N/A	-0.002	-0.216	0.235	0.083				758	0.28	0.28
Catotelm	1.093		-0.088	N/A	N/A	0.004	-0.286	0.688	0.147				775	0.41	0.41

[&] Number of measurements (n), model coefficient of determination (R^2), adjusted R^2 (R^2-adj)

325

3.1.2 $THg_{porewater}$ Concentration

The ANCOVA results indicated that log-transformed $THg_{porewater}$ concentration did not have a significant relationship with mean daily soil temperature for the full depth profile or the catotelm (Table 2). Within the acrotelm, log-transformed $THg_{porewater}$ did have a significant, positive relationship with mean daily soil temperature ($p < 0.001$, Table 2). When assessing individual depths (Figure 1), there was a significant relationship between mean daily soil temperature and $THg_{porewater}$ concentration in the top two depths (0 cm to -10 cm and -30 cm to -40 cm) which corresponds to the acrotelm. However, the R^2 values are low which indicates that temperature alone, while statistically significant, is not a good predictor. The deeper two depths (-50 cm to -60 cm and -100 cm to -110 cm) did not have a significant relationship between mean daily soil temperature and $THg_{porewater}$ concentration (Figure 1).

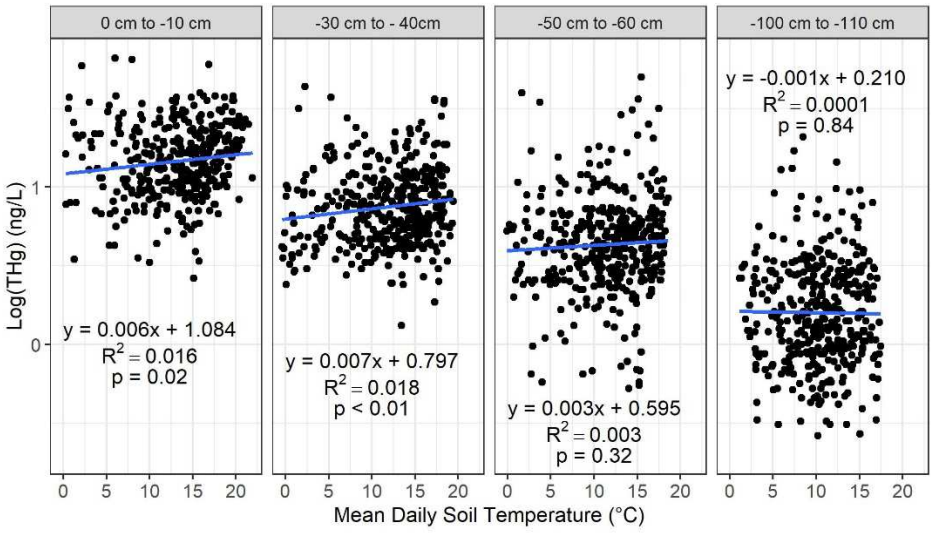

Fig. 1 *Linear regression of mean daily soil temperature with log-transformed $THg_{porewater}$ concentration split by depth increment. The depths 0 cm to -10 cm and -30 cm to -40 cm had significant p-values (< 0.05) and a positive slope. The depths -50 cm to -60 cm and -100 cm to -110 cm did not have significant p-values.*

The stepwise MLR of log-transformed $THg_{porewater}$ concentration resulted in an R^2 value of 0.64 with a significant p-value (< 0.0001) and included depth (cm), mean daily soil temperature measured at depth (°C), mean seasonal water table height (cm), pH, sulfate concentration (mg L^{-1}), and total iron concentration (mg L^{-1}). Porewater sulfate, iron, and acidity were all positively correlated with increased concentration of $THg_{porewater}$. For TOC concentrations, the relationship with $THg_{porewater}$ depended on the depth interval in the soil; there was a negative correlation in the acrotelm and a positive correlation in the catotelm. For the full depth profile, this analysis did not identify a simple relationship between TOC and $THg_{porewater}$. Temperature had a positive coefficient which indicates that as temperature increases,

346 log-transformed $THg_{porewater}$ concentration also increases (Table 3). When performing separate MLRs for the acrotelm
347 and catotelm, temperature had a positive coefficient with log-transformed $THg_{porewater}$ in the acrotelm and was not an
348 influential variable in the catotelm.

349 **3.1.3 Ratio of THg_{peat} to $THg_{porewater}$**

350 A negative relationship of -0.40 (Spearman's correlation analysis) was observed between THg_{peat}:$THg_{porewater}$ and the
351 mean daily soil temperature when considering the whole depth profile ($p < 0.0001$, Table S3 and Figure S3). When
352 analyzing the acrotelm (0 cm to -40 cm) only, the relationship was even stronger with a correlation coefficient of -
353 0.58 (Table S3). The catotelm (50 cm to -110 cm) did not show a significant relationship between mean daily soil
354 temperature and THg_{peat}:$THg_{porewater}$ (Table S3). The THg_{peat} to $THg_{porewater}$ ratio did not have a significant relationship
355 with pH in the acrotelm, but in the catotelm the relationship was positive (rho = 0.54, Table S3) indicating that as pH
356 decreased the partitioning of THg moved from the peat into the porewater. A negative relationship was observed
357 between THg_{peat}:$THg_{porewater}$ and aqueous sulfate, total dissolved iron, and TOC over the whole depth profile (rho = -
358 0.50, -0.42, and -0.37, respectively, Table S3). These relationships indicate that increases in these aqueous variables
359 were correlated with net partitioning of THg from the peat to the porewater. Curiously, the height of the water table
360 did not have a significant relationship with THg_{peat}:$THg_{porewater}$.

361 **3.2 Effect of Elevated Carbon Dioxide on THg Concentration**

362 The following subsections will cover the effects of elevated CO2 on THg_{peat} concentration, $THg_{porewater}$ concentration,
363 and THg_{peat}:$THg_{porewater}$.

364 **3.2.1 THg_{peat} Concentration**

365 The ANCOVA results demonstrated that log-transformed THg_{peat} concentrations were not different between the CO_2
366 levels (ambient and elevated, $p = 0.84$, Table 2). Additionally, ANCOVA analysis demonstrated that the interaction
367 of mean daily soil temperature and CO_2 treatment was not significant ($p = 0.96$, Table 2). The stepwise MLR of log-
368 transformed THg_{peat} concentrations resulted in an R^2 value of 0.60 with a significant p-value (<0.0001) and included
369 depth (cm), CO_2 treatment, mean seasonal water table height (cm), C:N, percent sulfur by weight, percent of ester
370 sulfate out of total sulfur, percent of sulfone/sulfonate, percent of sulfoxide, and percent of organic disulfide (Table
371 3). The elevated CO_2 treatment had a negative coefficient which indicates that at elevated CO_2, log-transformed
372 THg_{peat} concentration is less than at ambient CO_2 (Table 3).

373 **3.2.2 $THg_{porewater}$ Concentration**

Log-transformed $THg_{porewater}$ concentration was not different between the CO_2 levels when analyzing the full depth profile ($p = 0.07$, Table 2). There were differences in log-transformed $THg_{porewater}$ concentration when split into the acrotelm and catotelm (Table 2). In the acrotelm, the log-transformed $THg_{porewater}$ concentration was significantly higher in the elevated CO_2 enclosures ($p = 0.04$, Table S4). However, in the catotelm, the log-transformed $THg_{porewater}$ concentration was significantly higher in the ambient CO_2 enclosures ($p < 0.01$, Table S4). Assessing all four depth increments using ANCOVA (Figure 2), the shallowest and deepest depths sampled (0 cm to -10 cm and -100 cm to -110 cm) were not different between the CO_2 levels. The middle depths (-30 cm to -40 cm and -50 cm to -60 cm) were different between the CO_2 levels and matched what was seen in the acrotelm/catotelm. At -30 cm to -40 cm, the elevated CO_2 enclosures had significantly higher ($p < 0.0001$) $THg_{porewater}$ concentrations whereas at -50 cm to -60 cm, the elevated CO_2 enclosures had significantly lower $THg_{porewater}$ concentrations ($p < 0.0001$). The interaction of mean daily soil temperature and CO_2 level was not significant per an ANCOVA analysis ($p = 0.13$).

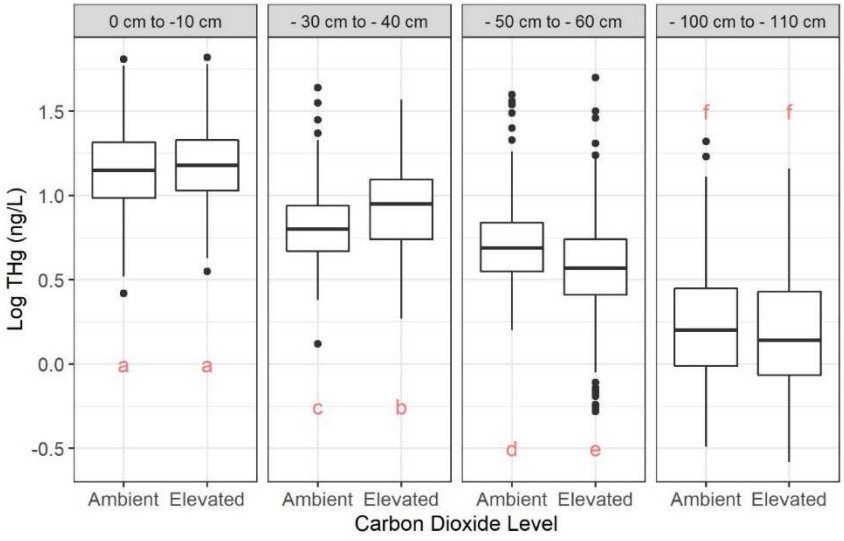

Fig. 2 *Box plots of log-transformed $THg_{porewater}$ concentration by carbon dioxide level and depth increment. Differences ($p < 0.05$) between CO_2 levels, determined from ANCOVA pairwise analyses, are shown by different letters. Letters are compared across depths. Log-transformed $THg_{porewater}$ concentrations were unaffected by elevated CO_2 conditions at the depth increment 0 cm to -10 cm. In depth increment -30 cm to -40 cm log-transformed $THg_{porewater}$ concentrations were enhanced in the elevated CO_2 enclosures. In the catotelm, log-transformed $THg_{porewater}$ concentrations were reduced in the elevated CO_2 enclosures at the depth increment -50 cm to -60 cm and log-transformed $THg_{porewater}$ concentrations were unaffected by elevated CO_2 conditions at the depth increment -100 cm to -110 cm.*

394 The stepwise MLR of log-transformed $THg_{porewater}$ concentration did not include CO_2 treatment as an important
395 variable when assessing the full depth profile. However, when the depth profile is split into the acrotelm and catotelm,
396 the elevated CO_2 treatment had a positive coefficient in the acrotelm and a negative coefficient in the catotelm (Table
397 3) indicating that at elevated CO_2, the log-transformed $THg_{porewater}$ concentration was higher in the acrotelm and lower
398 in the catotelm as compared to ambient CO_2. The stepwise MLRs for the acrotelm and catotelm had significant p-
399 values (both <0.0001) and R^2 values were 0.28 and 0.41, respectively (Table 3).

400 **3.3 Effect of Temperature and Carbon Dioxide on Water Table Height**

401 The ANCOVA analysis revealed that the height of the water table decreased with increasing temperature under both
402 CO_2 levels (Figure 3). The linear regression of mean daily soil temperature with daily water table height had negative
403 slopes for ambient CO_2 and elevated CO_2 (slope = -0.006 and -0.007, respectively, Figure 3). The ANCOVA analysis
404 demonstrated that the interaction of mean daily soil temperature and CO_2 level was significant ($p < 0.01$, Table 2).
405 This finding indicates the negative trend between mean daily soil temperature and daily water table was significantly
406 enhanced under elevated CO_2 conditions as the linear regression of mean daily soil temperature with daily water table
407 height had a more negative slope than under ambient CO_2 conditions (Figure 3). The mean daily water table height
408 was higher under elevated CO_2 conditions (Table S5).

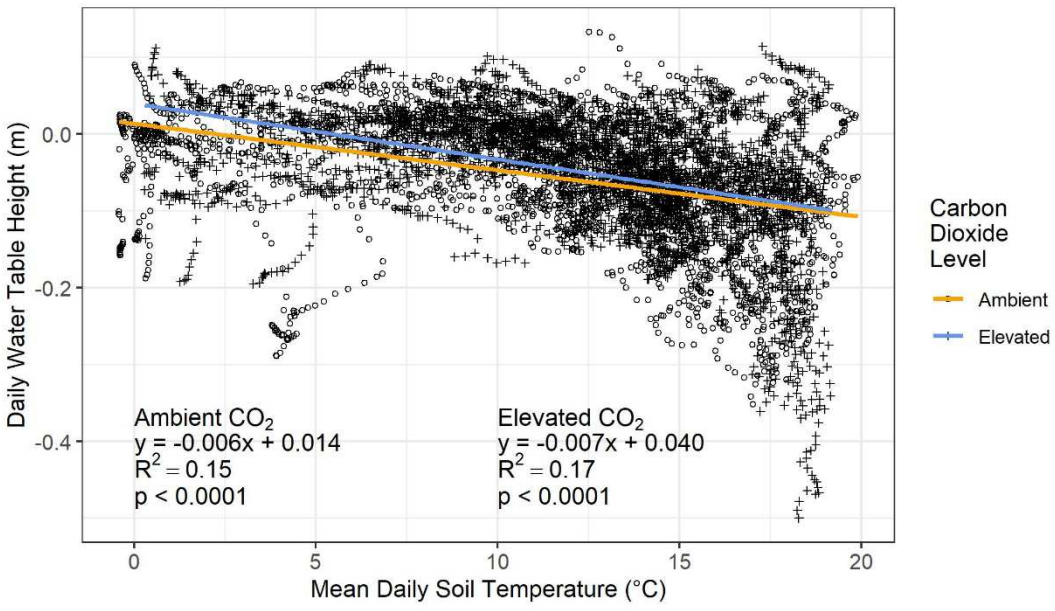

409

410 ***Fig. 3*** *Linear regression of mean daily soil temperature with daily water table height. The interaction of mean daily*
411 *soil temperature and CO_2 level was significant ($p < 0.01$, Table 2). The daily water table lowers in response to*

warming and this trend is enhanced at elevated CO_2. The mean water table height is higher under elevated CO_2 conditions than at ambient CO_2 conditions (Table S5)

A single linear regression of chloride concentration with mean daily soil temperature was significant ($p < 0.05$) but had a low R^2 value of 0.06 (Figure S4) indicating that evaporative concentration was not an important factor affecting $THg_{porewater}$ concentration. $Chloride_{porewater}$ concentration versus mean daily soil temperature relationships were analyzed by temperature treatment, and the slopes of these relationships were not significantly different from one another ($p = 0.32$, Figure S5). Total $mercury_{porewater}$ concentration versus chloride concentration relationships were analyzed by temperature treatment, and the slopes of these relationships were not significantly different from one another ($p = 0.92$, Figure S6).

3.4 Effect of Water Table on Peat and Porewater THg Concentration

The relationship between water table height and THg_{peat} concentration was positive (Table 3). In contrast, the relationship between water table height and $THg_{porewater}$ concentration was negative (Table 3). Water table height and THg_{peat}:$THg_{porewater}$ were not significantly correlated ($p = 0.068$, Table S3).

4. DISCUSSION

4.1 Effect of Temperature on THg Concentration

The THg_{peat} concentration did not show a response to temperature (Table 2 and Table 3). It is possibly too early in the 10-year SPRUCE experiment to measure effects as the results of this study only cover the first 3 years of the experiment. However, carbon, iron, and nitrogen cycling changes have been observed over that time period (Wilson et al. 2016, 2021a, b; Hanson et al. 2020; Curtinrich et al. 2022; Iversen et al. 2022). The $THg_{porewater}$ concentration increased with warming (Table 2 and Figure 1) likely because porewaters are more responsive to change than peat. Porewaters have been reported to be a sensitive indicator of metal mobilization in peat and chemical components can be more reactive in porewater than in peat (Bourbonniere 2009; Shotyk et al. 2016). Additionally, the mass of mercury in peat is much larger than the mass of mercury in porewater so proportionally greater changes are needed to observe an effect in the peat as compared to the porewater. In the top 100 cm, there is approximately 10^7 ng m^{-3} THg in peat and 10^2 ng m^{-3} THg in the porewater, a difference of 5 orders of magnitude (Supplemental Information, "Mass Balance Calculations").

The stepwise MLR of log-transformed THg_{peat} did not include the organic monosulfide group ("thiols, organic monosulfides, and thiophenes" or TMT, Table 3) as an influential group which was surprising given that mercury

has a demonstrated affinity with thiols (Skyllberg 2008; Nagy et al. 2011). However, organic disulfide (a reduced sulfur species, R-S-S-R') was included in the MLR and had a positive relationship (Table 3). Similar trends were seen in the Spearman's correlation analysis of THg_{peat}:$THg_{porewater}$. In peat, as the proportion of organic monosulfide species increased, THg_{peat}:$THg_{porewater}$ decreased (Table S3). This finding is consistent with the net movement of THg from peat to porewater at depths where organic monosulfides are most abundant. This negative relationship was also observed in the 2012 study of the initial conditions at the same site (Pierce et al. 2022). As the proportion of organic disulfide species increased in peat, THg_{peat}:$THg_{porewater}$ increased (Table S3), indicating retention of mercury where organic disulfide is present. Overall, the data indicate that peat with higher proportions of organic disulfide retain more THg in the solid phase than peat with higher proportions of organic monosulfide.

In the SPRUCE experiment, the $THg_{porewater}$ concentration increased as the temperature increased, primarily in the acrotelm (Table 3). Furthermore, the response of THg_{peat}:$THg_{porewater}$ to warming indicated that the partitioning of mercury shifted from the peat into the porewater as the temperature increased. In addition to mercury, dissolved sulfate, total dissolved iron, and acidity increased in porewaters. The increased concentration of $THg_{porewater}$ and other solutes is likely a result of more rapid decomposition of the peat at elevated temperatures. At the SPRUCE experiment, research has shown that in the first 3 years of the experiment, warming has caused a rate of carbon loss of 31.3 g $C \cdot m^{-2} \cdot year^{-1} \cdot °C^{-1}$ and was associated with peat decomposition and declining peat elevation (Hanson et al. 2020). Previous studies have shown that decomposition of sedimentary organic matter in freshwater wetlands leads to mobilization of mercury into porewaters (Myrbo et al. 2017). A negative relationship (Table S3) between TOC and THg_{peat}:$THg_{porewater}$ was observed. This indicates as TOC concentrations increased in porewater, there was a partitioning of mercury from the peat into the porewater. Increased TOC concentrations in porewater is consistent with peat decomposition and supports our interpretation that increased mercury in the porewaters is related to decomposition. Using stepwise MLR analysis, we observed that within the acrotelm a positive relationship (Table 3) was observed between $THg_{porewater}$ concentration and porewater TOC concentration. This finding is also consistent with the interpretation that at depths where peat decomposes to release TOC to porewaters, there is also release of mercury and other solutes to porewater.

Another source of mercury to the porewaters is atmospheric deposition but, given the close proximity of the enclosures, deposition is likely equal across treatments (Figures S1 and S2). The annual open air THg atmospheric wet deposition at the nearby (2.5 km) MEF Mercury Deposition Network site was 6.9 μg m^{-2}, 8.6 μg m^{-2}, and 7.1 μg

468 m^{-2} for the years 2017, 2018, and 2019, respectively (National Atmospheric Deposition Program 2018, 2019, 2020).
469 Evaporative concentration is addressed in section 4.4 and determined not to be an influential factor on $THg_{porewater}$
470 concentrations.

471 **4.2 Effect of Carbon Dioxide on THg Concentration**

472 Elevated CO_2 did not affect THg_{peat} concentration in the ANCOVA analysis (Table 2). However, the stepwise MLR
473 showed a negative relationship between elevated CO_2 and THg_{peat} concentration (Table 3). To our knowledge there
474 are no previous investigations in which a negative relationship between CO_2 and THg concentration has been
475 observed. Within the acrotelm, elevated CO_2 concentration led to increased $THg_{porewater}$ concentration whereas in the
476 catotelm it led to decreased $THg_{porewater}$ concentration (Table 3 and Figure 2). The positive relationship in the acrotelm
477 was due primarily to the -30 cm to -40 cm depth increment (Figure 2) which is in the typical zone of water table
478 fluctuation

479 Past studies have shown that elevated CO_2 had a positive effect on the growth of certain vegetation types, such as
480 sedges, in peatlands (Fenner et al. 2007; Dieleman et al. 2015). Sedges, a vascular plant, have been observed to
481 increase peat mercury accumulation because of mercury translocation from the plant to the soil (Haynes et al. 2017b).
482 The increase in sedge vegetation or changes in root exudates could be related to the increase in $THg_{porewater}$
483 concentration seen in the acrotelm. However, published research from the SPRUCE experiment have only shown
484 limited effects of elevated CO_2 on the plant community and physiology (Hanson et al. 2020; Malhotra et al. 2020;
485 McPartland et al. 2020; Iversen et al. 2022). For THg concentrations in porewaters, the overall effect of CO_2 is subtle
486 and likely indirect through effects on plant evapotranspiration and water table height.

487 **4.3 Effect of Temperature and Carbon Dioxide on the Water Table Height**

488 In an ecosystem, such as a peatland, where water is not limiting, increased temperature will cause an increase in the
489 rate of evapotranspiration, an important part of the water cycle (Maček et al. 2018; Zhang and Wang 2021).
490 Increased evapotranspiration leads to a lowering of the water table in peatlands. A recent SPRUCE modeling study
491 demonstrated evaporation and transpiration to be important drivers of the water table height in peatlands (Yuan et al.
492 2021). As expected, water table height in the SPRUCE experiment decreased as temperature increased (Figure 3,
493 Hanson et al. 2020). This relationship has been demonstrated in other experiments in peatlands (Roulet et al. 1992;
494 Moore et al. 1998). There was a significant interaction effect (Table 2) between mean daily soil temperature and
495 CO_2 level on water table height. Both CO_2 levels had a negative relationship between mean daily soil temperature

and daily water table height (Figure 3). Under elevated CO_2 conditions this negative relationship was amplified as compared to ambient CO_2 conditions (Figure 3). A caveat to this data is that we suspect that the enclosure with +9 °C treatment and ambient CO_2 had external water ingress (when water levels outside of the enclosure were high) due to a persistent mechanical challenge in sealing the below-ground corral. It is possible that the +9 °C treatment with ambient CO_2 had an artificially high water table. In contrast, the corresponding +9 °C treatment with elevated CO_2 did not have perceptible leakage.

We expected that elevated CO_2 would cause increased primary productivity in plants which would lower the water table (Norby et al. 2010; Reyer et al. 2014). However, the elevated CO_2 treatment had a higher mean daily water table than the ambient CO_2 level (Table S5). This finding was more pronounced at lower temperatures and less pronounced at warmer temperatures (Figure 3). Higher water tables could be caused by plant stomata closing as a response to elevated CO_2 and limiting transpiration. Studies in vascular plants found that elevated CO_2 caused reductions in stomatal density, stomatal conductance, leaf transpiration, and ecosystem evapotranspiration (De Kauwe et al. 2013; Xu et al. 2016). However, in the SPRUCE experiment, only minimal effects of CO_2 were observed on vascular plants (McPartland et al. 2020). *Sphagnum* moss, which is not a vascular plant and does not have stomata, had lower productivity in the elevated CO_2 treatment likely due to increased shading by shrubs (Shi et al. 2015; Norby et al. 2019). At the SPRUCE site, warming was associated with an increase in above-ground vascular plant biomass and a decrease in *Sphagnum* moss cover (Norby et al. 2019; McPartland et al. 2020). With an increase in vascular plant coverage and a decrease *Sphagnum* moss cover, stomatal regulation by CO_2 may become more important in this system with potential effects on water table height.

4.4 Effect of Water table on THg Concentration

For the SPRUCE experiment, a lower water table was associated with increased $THg_{porewater}$ concentration and decreased THg_{peat} concentration (Table 3). Decreased water table heights associated with increased temperature, exposes more peat to oxic conditions which likely leads to more rapid decomposition and release of THg_{peat} to porewater. A mesocosm study found that lowering the water table resulted in mercury mobilization from peat into porewaters due to increased peat decomposition (Haynes et al. 2017a, 2019).

It is unlikely that $THg_{porewater}$ concentration increased due to evaporative concentration because $chloride_{porewater}$ concentration was not related to water table height (Figure S4), the slopes of the simple linear regression of $chloride_{porewater}$ concentration with mean daily soil temperature did not vary among temperature treatments (Figure

S5), and the slopes of the simple linear regression of $THg_{porewater}$ concentration and $chloride_{porewater}$ concentration did not vary among the temperature treatments (Figure S6). These findings indicate that warming did not affect the relationship of $THg_{porewater}$ to $chloride_{porewater}$. Evaporative concentration has been found to be minimally important in this and other bogs (Griffiths and Sebestyen 2016b; Haynes et al. 2017a; Curtinrich et al. 2022). It is possible that evaporative concentration is relevant on the scale of hundreds of years but in the scope of this relatively short-term study (3 years), evaporative concentration does not appear to be affecting porewater solute concentrations due to the temperature treatment.

CONCLUSION

At the outset of this study, we expected that increases in temperature (soil and air) in the northern boreal ecotone would increase mercury release from peat to porewaters. After three years of experimental treatment, our findings have shown that increased temperature was correlated with a lower water table height and increased THg in peatland porewaters. We also observed that porewaters are more likely to have measurable changes in THg than peat. The response of THg to temperature and CO_2 changed with depth in the peatland. Elevated atmospheric CO_2 concentrations were correlated with a decrease in THg_{peat} concentration and an increase in $THg_{porewater}$ concentration in the surface layer of peat (acrotelm). Increased mercury concentration in porewaters may be available for export to surface water where it may be methylated and biomagnify in the aquatic food web. Peatlands have historically been sinks of atmospherically derived mercury but also sources to downstream water bodies. Further investigation of mercury fluxes to the atmosphere and in outflow waters is needed to assess if the balance is shifting from a net sink to a net source under climate change. In the first three years of this 10-year study with elevated temperature and CO_2 treatments, the response was significant but subtle. This is an overall positive result for the local aquatic environment as the increases in mercury related to warming and CO_2 are small.

DATA AVAILABILITY

The data in this manuscript can be accessed in the following repositories.

Griffiths, N. A., S.D. Sebestyen, K.C. Oleheiser, J.M. Stelling, C.E. Pierce, E.A. Nater, B.M. Toner, & R.K. Kolka. (2016) SPRUCE Porewater Chemistry Data for Experimental Plots, Beginning in 2013. Oak Ridge National Laboratory, TES SFA, US Department of Energy, Oak Ridge, Tennessee, USA. Version 3. https://doi.org/10.3334/CDIAC/spruce.028.

Hanson, P.J., J.S. Riggs, W.R. Nettles, M.B. Krassovski, and L.A. Hook. (2016) SPRUCE Whole Ecosystems Warming (WEW) Environmental Data Beginning August 2015. Oak Ridge National Laboratory, TES SFA, U.S. Department of Energy, Oak Ridge, Tennessee, U.S.A. https://doi.org/10.3334/CDIAC/spruce.032

Hanson, P.J., Phillips, J.R., Nettles, W.R., Pearson, K.J., Hook, L.A. (2020) SPRUCE Plot-Level Water Table Data Assessments for Absolute Elevations and Height with Respect to Mean Hollows Beginning in 2015. Oak Ridge National Laboratory, TES SFA, U.S. Department of Energy, Oak Ridge, Tennessee, U.S.A. https://doi.org/10.25581/spruce.079/1608615

Pierce C.E., Psarska S., Brozowski J., Sebestyen S.D., Kolka R.K., Gutknecht J.L.M., Nater E.A., Toner B.M. (2022) SPRUCE Peat Mercury, Methylmercury and Sulfur Concentrations from Experimental Plot Cores, Beginning in 2014. Oak Ridge National Laboratory, TES SFA, U.S. Department of Energy, Oak Ridge, Tennessee, U.S.A. https://doi.org/10.25581/spruce.074/1579555

REFERENCES

Amos HM, Jacob DJ, Streets DG, Sunderland EM (2013) Legacy impacts of all-time anthropogenic emissions on the global mercury cycle. Global Biogeochem Cycles 27:410–421. https://doi.org/10.1002/gbc.20040

Andersen R, Chapman SJ, Artz RRE (2013) Microbial communities in natural and disturbed peatlands: A review. Soil Biol Biochem 57:979–994. https://doi.org/10.1016/j.soilbio.2012.10.003

APHA (2017) Standard methods for the examination of water and wastewater, 23rd edn. American Public Health Association, Washington DC, USA

Benoit JM, Gilmour CC, Heyes A, et al (2003) Geochemical and biological controls over methylmercury production and degradation in aquatic ecosystems. ACS Symp 835:1–33. https://doi.org/10.1021/bk-2003-0835.ch019

Bloom NS, Crecelius EA (1983) Determination of mercury in seawater at sub-nanogram per liter levels. Mar Chem 14:49–59

Bottrell S, Novak M (1997) Sulphur Isotopic Study of Two Pristine Sphagnum Bogs in the Western British Isles. J Ecol 85:125–132

Bourbonniere RA (2009) Review of water chemistry research in natural and disturbed peatlands. Can Water Resour J 34:393–414. https://doi.org/10.4296/cwrj3404393

Bravo AG, Peura S, Buck M, et al (2018) Methanogens and iron-reducing bacteria: The overlooked members of mercury-methylating microbial communities in boreal lakes. Appl Environ Microbiol 84:1–16. https://doi.org/10.1128/AEM.01774-18

Clarkson TW, Magos L (2006) The toxicology of mercury and its chemical compounds. Crit Rev Toxicol 36:609–662. https://doi.org/10.1080/10408440600845619

Coleman Wasik JK, Mitchell CPJJ, Engstrom DR, et al (2012) Methylmercury declines in a boreal peatland when experimental sulfate deposition decreases. Environ Sci Technol 46:6663–6671. https://doi.org/10.1021/es300865f

Cottingham KL, Lennon JT, Brown BL (2005) Knowing when to draw the line: designing more informative ecological experiments. Front Ecol Environ 3:145–152. https://doi.org/10.1890/1540-9295(2005)003[0145:KWTDTL]2.0.CO;2

Cron BR, Sheik CS, Kafantaris FCA, et al (2020) Dynamic Biogeochemistry of the Particulate Sulfur Pool in a Buoyant Deep-Sea Hydrothermal Plume. ACS Earth Sp Chem 4:168–182. https://doi.org/10.1021/acsearthspacechem.9b00214

Curtinrich HJ, Sebestyen SD, Griffiths NA, Hall SJ (2022) Warming Stimulates Iron-Mediated Carbon and Nutrient Cycling in Mineral-Poor Peatlands. Ecosystems 25:44–60. https://doi.org/10.1007/s10021-021-00639-3

De Kauwe MG, Medlyn BE, Zaehle S, et al (2013) Forest water use and water use efficiency at elevated CO2: a

595 model-data intercomparison at two contrasting temperate forest FACE sites. Glob Chang 19:1759–1779.
596 https://doi.org/10.1111/gcb.12164

597 de Mendiburu F, Yaseen M (2020) agricolae: Statistical Procedures for Agricultural Research

598 Dieleman CM, Branfireun BA, Mclaughlin JW, Lindo Z (2015) Climate change drives a shift in peatland ecosystem
599 plant community: Implications for ecosystem function and stability. Glob Chang Biol 21:388–395.
600 https://doi.org/10.1111/gcb.12643

601 Driscoll CT, Mason RP, Chan HM, et al (2013) Mercury as a global pollutant: Sources, pathways, and effects.
602 Environ Sci Technol 47:4967–4983. https://doi.org/10.1021/es305071v

603 Feng X, Deventer MJ, Lonchar R, et al (2020) Climate Sensitivity of Peatland Methane Emissions Mediated by
604 Seasonal Hydrologic Dynamics. Geophys Res Lett 47:1–9. https://doi.org/10.1029/2020GL088875

605 Fenner N, Freeman C, Lock MA, et al (2007) Interactions between elevated CO2 and warming could amplify DOC
606 exports from peatland catchments. Environ Sci Technol 41:3146–3152. https://doi.org/10.1021/es061765v

607 Fox J, Weisberg S (2019) An R Companion to Applied Regression, 3rd edn. Sage, Thousand Oaks CA

608 Gabriel MC, Kolka R, Wickman T, et al (2009) Evaluating the spatial variation of total mercury in young-of-year
609 yellow perch (Perca flavescens), surface water and upland soil for watershed-lake systems within the southern
610 Boreal Shield. Sci Total Environ 407:4117–4126. https://doi.org/10.1016/j.scitotenv.2009.03.019

611 Gordon J, Quinton W, Branfireun BA, Olefeldt D (2016) Mercury and methylmercury biogeochemistry in a thawing
612 permafrost wetland complex, Northwest Territories, Canada. Hydrol Process 30:3627–3638.
613 https://doi.org/10.1002/hyp.10911

614 Gorham E (1991) Northern peatlands: Role in the carbon cycle and probably responses to climatic warming. Ecol
615 Appl 1:182–195

616 Griffiths NA, Sebestyen SD (2016a) SPRUCE Porewater Chemistry Data for Experimental Plots Beginning in 2013.
617 Oak Ridge, TN Carbon Dioxide Inf Anal Center, Oak Ridge Natl Lab US Dep Energy 1–15.
618 https://doi.org/10.3334/CDIAC/spruce.028

619 Griffiths NA, Sebestyen SD (2016b) Dynamic Vertical Profiles of Peat Porewater Chemistry in a Northern Peatland.
620 Wetlands 36:1119–1130. https://doi.org/10.1007/s13157-016-0829-5

621 Grigal DF (2003) Mercury sequestration in forests and peatlands: a review. J Environ Qual 32:393–405.
622 https://doi.org/10.2134/jeq2003.3930

623 Grigal DF, Kolka RK, Fleck JA, Nater EA (2000) Mercury budget of an upland-peatland watershed.
624 Biogeochemistry 50:95–109

625 Hanson PJ, Griffiths NA, Iversen CM, et al (2020) Rapid Net Carbon Loss From a Whole - Ecosystem Warmed
626 Peatland. AGU Adv 1:1–18. https://doi.org/10.1029/2020AV000163

627 Hanson PJ, Riggs JS, Robert Nettles W, et al (2017) Attaining whole-ecosystem warming using air and deep-soil
628 heating methods with an elevated CO2 atmosphere. Biogeosciences 14:861–883. https://doi.org/10.5194/bg-
629 14-861-2017

630 Haynes KM, Kane ES, Potvin L, et al (2017a) Mobility and transport of mercury and methylmercury in peat as a
631 function of changes in water table regime and plant functional groups. Global Biogeochem Cycles 31:233–
632 244. https://doi.org/10.1002/2016GB005471

633 Haynes KM, Kane ES, Potvin L, et al (2017b) Gaseous mercury fluxes in peatlands and the potential influence of
634 climate change. Atmos Environ 154:247–259. https://doi.org/10.1016/j.atmosenv.2017.01.049

635 Haynes KM, Kane ES, Potvin L, et al (2019) Impacts of experimental alteration of water table regime and vascular
636 plant community composition on peat mercury profiles and methylmercury production. Sci Total Environ
637 682:611–622. https://doi.org/10.1016/j.scitotenv.2019.05.072

638 Hilbert DW, Roulet N, Moore T (2000) Modelling and analysis of peatlands as dynamical systems. J Ecol 88:230–
639 242. https://doi.org/10.1046/j.1365-2745.2000.00438.x

640 Holm S (1979) A simple sequentially rejective multiple test procedure. Scand J Stat 6:65–70

641 Hu H, Wang B, Bravo AG, et al (2020) Shifts in mercury methylation across a peatland chronosequence: From
642 sulfate reduction to methanogenesis and syntrophy. J Hazard Mater 387:1–9.
643 https://doi.org/10.1016/j.jhazmat.2019.121967

644 Inskip MJ, Piotrowski JK, Indript MJ, Piotrowskis JK (1985) Review of the health effects of methylmercury. J Appl
645 Toxicol 5:113–33. https://doi.org/10.1002/jat.2550050302

646 IPCC (2021) Summary for Policy Makers. Cambridge University Press, Cambridge, United Kingdom

647 Ise T, Dunn AL, Wofsy SC, Moorcroft PR (2008) High sensitivity of peat decomposition to climate change through
648 water-table feedback. Nat Geosci 1:763–766. https://doi.org/10.1038/ngeo331

649 Iversen CM, Hansen P, Brice DJ, et al (2014) SPRUCE Peat Physical and Chemical Characteristics from
650 Experimental Plot Cores , 2012. Carbon Dioxide Inf Anal Center, Oak Ridge Natl Lab US Dep Energy, Oak
651 Ridge, Tennessee, USA

652 Iversen CM, Latimer J, Brice DJ, et al (2022) Whole-Ecosystem Warming Increases Plant-Available Nitrogen and
653 Phosphorus in an Ombrotrophic Bog. Ecosystems. https://doi.org/10.1007/s10021-022-00744-x

654 Jowsey PC (1966) An improved peat sampler. New Phytol 65:245–248

655 Lenth R V. (2022) emmeans: Estimated Marginal Means, aka Least-Squares Means

656 Li F, Ma C, Zhang P (2020) Mercury Deposition, Climate Change and Anthropogenic Activities: A Review. Front
657 Earth Sci 8:1–17. https://doi.org/10.3389/feart.2020.00316

658 Lindberg S, Bullock R, Ebinghaus R, et al (2007) A synthesis of progress and uncertainties in attributing the sources
659 of mercury in deposition. A J Hum Environ 36:19–33. https://doi.org/10.1579/0044-
660 7447(2007)36[19:ASOPAU]2.0.CO;2

661 Ma Z, Peng C, Zhu Q, et al (2012) Regional drought-induced reduction in the biomass carbon sink of Canada's
662 boreal forests. PNAS 109:2423–2427. https://doi.org/10.1073/pnas.1111576109

663 Maček U, Bezak N, Šraj M (2018) Reference evapotranspiration changes in Slovenia, Europe. Agric For Meteorol
664 260–261:183–192. https://doi.org/10.1016/j.agrformet.2018.06.014

665 Malhotra A, Brice DJ, Childs J, et al (2020) Peatland warming strongly increases fine-root growth. PNAS
666 117:17627–17634. https://doi.org/10.1073/pnas.2003361117

667 Manceau A, Nagy KL (2012) Quantitative analysis of sulfur functional groups in natural organic matter by XANES
668 spectroscopy. Geochim Cosmochim Acta 99:206–223. https://doi.org/10.1016/j.gca.2012.09.033

669 McPartland MY, Montgomery RA, Hanson PJ, et al (2020) Vascular plant species response to warming and elevated
670 carbon dioxide in a boreal peatland. Environ Res Lett 15:1–12. https://doi.org/doi.org/10.1088/1748-
671 9326/abc4fb

672 Meili M (1991) The coupling of mercury and organic matter in the biogeochemical cycle — towards a mechanistic
673 model for the boreal forest zone. Water Air Soil Pollut 56:333–347. https://doi.org/10.1007/BF00342281

674 Mitchell CPJ, Branfireun BA, Kolka RK (2008a) Spatial characteristics of net methylmercury production hot spots
675 in peatlands. Environ Sci Technol 42:1010–1016. https://doi.org/10.1021/es0704986

676 Mitchell CPJ, Branfireun BA, Kolka RK (2008b) Assessing sulfate and carbon controls on net methylmercury
677 production in peatlands: An in situ mesocosm approach. Appl Geochemistry 23:503–518.
678 https://doi.org/10.1016/j.apgeochem.2007.12.020

679 Moore TM, Roulet NT, Waddington JM (1998) Uncertainty In Predicting The Effect of Climatic Change on the
680 Carbon Cycling of Nothern Peatlands. Clim Change 40:229–245. https://doi.org/10.1023/A:1005408719297

681 Myrbo A, Swain EB, Johnson NW, et al (2017) Increase in Nutrients, Mercury, and Methylmercury as a
682 Consequence of Elevated Sulfate Reduction to Sulfide in Experimental Wetland Mesocosms. J Geophys Res
683 Biogeosciences 122:1–17. https://doi.org/10.1002/2017JG003788

684 Nagy KL, Manceau A, Gasper JD, et al (2011) Metallothionein-like multinuclear clusters of mercury(II) and sulfur
685 in peat. Environ Sci Technol 45:7298–7306. https://doi.org/10.1021/es201025v

686 National Atmospheric Deposition Program (2018) National Atmospheric Deposition Program 2017 Annual
687 Summary

688 National Atmospheric Deposition Program (2019) National Atmospheric Deposition Program 2018 Annual
689 Summary

690 National Atmospheric Deposition Program (2020) National Atmospheric Deposition Program 2019 Annual
691 Summary

692 Nicholas SL, Erickson ML, Woodruff LG, et al (2017) Solid-phase arsenic speciation in aquifer sediments: A micro-
693 X-ray absorption spectroscopy approach for quantifying trace-level speciation. Geochim Cosmochim Acta
694 211:228–255. https://doi.org/10.1016/j.gca.2017.05.018

695 Norby RJ, Childs J, Hanson PJ, Warren JM (2019) Rapid loss of an ecosystem engineer : Sphagnum decline in an
696 experimentally warmed bog. Ecol Evol 9:12571–12585. https://doi.org/10.1002/ece3.5722

697 Norby RJ, Warren JM, Iversen CM, et al (2010) CO2 enhancement of forest productivity constrained by limited
698 nitrogen availability. Proc Natl Acad Sci U S A 107:19368–19373. https://doi.org/10.1073/pnas.1006463107

699 Nungesser MK (2003) Modelling microtopography in boreal peatlands: hummocks and hollows. Ecol Modell
700 165:175–207. https://doi.org/10.1016/S0304-3800(03)00067-X

701 O'Connor D, Hou D, Ok YS, et al (2019) Mercury speciation, transformation, and transportation in soils,
702 atmospheric flux, and implications for risk management: A critical review. Environ Int 126:747–761.
703 https://doi.org/10.1016/j.envint.2019.03.019

704 Osgood A, Brahmstedt ES, Windle MJS, et al (2022) Proximity to Riparian Wetlands Increases Mercury Burden in
705 Fish in the Upper St. Lawrence River. Water 14:1–9. https://doi.org/10.3390/w14010070

706 Osterwalder S, Bishop K, Alewell C, et al (2017) Mercury evasion from a boreal peatland shortens the timeline for
707 recovery from legacy pollution. Nat Sci Reports 7:1–9. https://doi.org/10.1038/s41598-017-16141-7

708 Outridge PM, Mason RP, Wang F, et al (2018) Updated Global and Oceanic Mercury Budgets for the United
709 Nations Global Mercury Assessment 2018. Environ Sci Technol 52:11466–11477.
710 https://doi.org/10.1021/acs.est.8b01246

711 Parsekian AD, Slater L, Nolan J, et al (2012) Uncertainty in Peat Volume and Soil Carbon Estimated Using Ground-
712 Penetrating Radar and Probing. Soil Sci Soc Am J 76:1911–1918. https://doi.org/10.2136/sssaj2012.0040

713 Pierce CE, Furman OS, Nicholas SL, et al (2022) Role of Ester Sulfate and Organic Disulfide in Mercury
714 Methylation in Peatland Soils. Environ Sci Technol 56:1433–1444. https://doi.org/10.1021/acs.est.1c04662

715 Post WM, Pastor J, Zinke PJ, Stangenberger AG (1985) Global patterns of soil nitrogen storage. Nature 317:613–
716 616. https://doi.org/10.1038/317613a0

717 R Core Team (2017) R: A language and environment for statistical computing. R A Lang. Environ. Stat. Comput.

718 Ravel B, Newville M (2005) ATHENA, ARTEMIS, HEPHAESTUS: Data analysis for X-ray absorption
719 spectroscopy using IFEFFIT. J Synchrotron Radiat 12:537–541. https://doi.org/10.1107/S0909049505012719

720 Reyer C, Lasch-Born P, Suckow F, et al (2014) Projections of regional changes in forest net primary productivity for
721 different tree species in Europe driven by climate change and carbon dioxide. Ann For Sci 71:211–225.
722 https://doi.org/10.1007/s13595-013-0306-8

723 Roulet N, Moore T, Bubier J, Lafleur P (1992) Northern Fens: Methane Flux and Climatic Change. Tellus B Chem
724 Phys Meteorol 44:100–105. https://doi.org/10.3402/tellusb.v44i2.15429

725 Sanderman J, Amundson R (2003) Treatise on Geochemistry. In: Holland HD, Turekian KK (eds) Treatise on
726 Geochemistry. Elsevier Science Direct, Amsterdam, NED, pp 249–316

727 Sebestyen SD, Dorrance C, Olson DM, et al (2011) Long-term monitoring sites and trends at the Marcell
728 Experimental Forest. In: Kolka RK, Sebestyen SD, Verry ES, Brooks KN (eds) Peatland biogeochemistry and
729 watershed hydrology at the Marcell Experimental Forest. CRC Press, Boca Raton, FL, pp 15–71

730 Sebestyen SD, Funke MM, Cotner JB, et al (2020) Water chemistry data for studies of the biodegradability of
731 dissolved organic matter in peatland catchments at the Marcell Experimental Forest: 2009-2011, 2nd edn.
732 Forest Service Research Data Archive, Fort Collins, CO, USA

733 Sebestyen SD, Griffiths NA (2016) SPRUCE Enclosure Corral and Sump System: Description, Operation, and
734 Calibration. 1–26

735 Sebestyen SD, Lany NK, Roman DT, et al (2021) Hydrological and meteorological data from research catchments at
736 the Marcell Experimental Forest. Hydrol Process 35:e14092:1–9. https://doi.org/10.1002/hyp.14092

737 Selin NE (2009) Global Biogeochemical Cycling of Mercury: A Review. Annu Rev Environ Resour 34:43–63.
738 https://doi.org/10.1146/annurev.environ.051308.084314

739 Shi X, Thornton PE, Ricciuto DM, et al (2015) Representing northern peatland microtopography and hydrology
740 within the Community Land Model. Biogeosciences 12:6463–6477. https://doi.org/10.5194/bg-12-6463-2015

741 Shotyk W, Rausch N, Nieminen TM, et al (2016) Isotopic Composition of Pb in Peat and Porewaters from Three
742 Contrasting Ombrotrophic Bogs in Finland: Evidence of Chemical Diagenesis in Response to Acidification.
743 Environ Sci Technol 50:9943–9951. https://doi.org/10.1021/acs.est.6b01076

744 Simonin HA, Loukmas JJ, Skinner LC, Roy KM (2008) Lake variability: Key factors controlling mercury
745 concentrations in New York State fish. Environ Pollut 154:107–115.
746 https://doi.org/10.1016/j.envpol.2007.12.032

747 Skyllberg U (2008) Competition among thiols and inorganic sulfides and polysulfides for Hg and MeHg in wetland
748 soils and sediments under suboxic conditions: Illumination of controversies and implications for MeHg net
749 production. J Geophys Res 113:1–14. https://doi.org/10.1029/2008JG000745

750 Skyllberg U, Qian J, Frech W, et al (2003) Distribution of mercury, methyl mercury and organic sulphur species in
751 soil, soil solution and stream of a boreal forest catchment. Biogeochemistry 64:53–76.
752 https://doi.org/10.1023/A:1024904502633

753 Stevens JP (2013) Intermediate Statistics: A Modern Approach, 3rd edn. Routledge, New York, NY

754 Tfaily MM, Cooper WT, Kostka JE, et al (2014) Organic matter transformation in the peat column at Marcell
755 Experimental Forest: Humification and vertical stratification. J Geophys Res Biogeosciences 119:661–675.

https://doi.org/10.1002/2015JG002993

U.S. Environmental Protection Agency (2002) Method 1631, Revision E: Mercury in water by oxidation, purge and trap, and cold vapor atomic fluorescence spectrometry. EPA 821-R-96-012 1–46

Ullrich SM, Tanton TW, Abdrashitova SA (2001) Mercury in the aquatic environment: A review of factors affecting methylation. Crit Rev Environ Sci Technol 31:241–293. https://doi.org/10.1080/20016491089226

Urban N, Verry ES, Eisenreich S, et al (2011) Element Cycling in Upland/Peatland Watersheds. In: Kolka RK, Sebestyen SD, Verry ES, Brooks KN (eds) Peatland Biogeochemistry and Watershed Hydrology at the Marcell Experimental Forest. CRC Press, Boca Raton, FL, pp 213–233

Verry ES, Boelter DH, Päivänen J, et al (2011a) Physical Properties of Organic Soils. In: Kolka RK, Sebestyen SD, Verry ES, Brooks KN (eds) Peatland Biogeochemistry and Watershed Hydrology at the Marcell Experimental Forest. CRC Press, Boca Raton, FL, pp 135–176

Verry ES, Brooks KN, Nichols DS, et al (2011b) Watershed Hydrology. In: Kolka RK, Sebestyen SD, Verry ES, Brooks KN (eds) Peatland Biogeochemistry and Watershed Hydrology at the Marcell Experimental Forest. CRC Press, Boca Raton, FL, pp 193–212

Wang B, Nilsson MB, Eklöf K, et al (2020) Opposing spatial trends in methylmercury and total mercury along a peatland chronosequence trophic gradient. Sci Total Environ 718:1–9. https://doi.org/10.1016/j.scitotenv.2020.137306

Wang B, Zhong S, Bishop K, et al (2021) Biogeochemical influences on net methylmercury formation proxies along a peatland chronosequence. Geochim Cosmochim Acta 308:188–203. https://doi.org/10.1016/j.gca.2021.06.010

Wilson RM, Griffiths NA, Visser A, et al (2021a) Radiocarbon Analyses Quantify Peat Carbon Losses With Increasing Temperature in a Whole Ecosystem Warming Experiment. J Geophys Res Biogeosciences 126:1–17. https://doi.org/10.1029/2021JG006511

Wilson RM, Hopple AM, Tfaily MM, et al (2016) Stability of peatland carbon to rising temperatures. Nat Commun 7:13723. https://doi.org/10.1038/ncomms13723

Wilson RM, Tfaily MM, Kolton M, et al (2021b) Soil metabolome response to whole-ecosystem warming at the spruce and peatland responses under changing environments experiment. Proc Natl Acad Sci U S A 118:1–11. https://doi.org/10.1073/pnas.2004192118

Xu J, Liem-Nguyen V, Buck M, et al (2021) Mercury Methylating Microbial Community Structure in Boreal Wetlands Explained by Local Physicochemical Conditions. Front Environ Sci 8:1–14. https://doi.org/10.3389/fenvs.2020.518662

Xu Z, Jiang Y, Jia B, Zhou G (2016) Elevated-CO2 response of stomata and its dependence on environmental factors. Front Plant Sci 7:1–15. https://doi.org/10.3389/fpls.2016.00657

Yang Y kui, Zhang C, Shi X jun, et al (2007) Effect of organic matter and pH on mercury release from soils. J Environ Sci 19:1349–1354. https://doi.org/10.1016/S1001-0742(07)60220-4

Yu L, Zhong S, Pei L, et al (2016) Contribution of large-scale circulation anomalies to changes in extreme precipitation frequency in the United States. Environ Res Lett 11:1–8. https://doi.org/10.1088/1748-9326/11/4/044003

Yu ZC (2012) Northern peatland carbon stocks and dynamics: a review. Biogeosciences 9:4071–4085. https://doi.org/10.5194/bg-9-4071-2012

Yuan F, Wang Y, Ricciuto DM, et al (2021) Hydrological feedbacks on peatland CH4 emission under warming and elevated CO2: A modeling study. J Hydrol 603:1–12. https://doi.org/10.1016/j.jhydrol.2021.127137

798 Zeng T, Arnold WA, Toner BM (2013) Microscale Characterization of Sulfur Speciation in Lake Sediments.
799 Environ Sci Technol 47:1287–1296. https://doi.org/10.1021/es303914q

800 Zhang H, Wang L (2021) Analysis of the variation in potential evapotranspiration and surface wet conditions in the
801 Hancang River Basin, China. Nat Sci Reports 11:1–10. https://doi.org/10.1038/s41598-021-88162-2

802 Zhang Y, Jaegle L, Thompson L, Streets DG (2014) Six centuries of changing oceanic mercury. Global Biogeochem
803 Cycles 28:1251–1261. https://doi.org/10.1111/1462-2920.13280

804

805 **STATEMENTS AND DECLARATIONS**

806 **Funding**

807 Funding from the National Science Foundation Graduate Fellowship Program supported Caroline E. Pierce. The
808 SPRUCE experiment and Natalie A. Griffiths are supported by the U.S. Department of Energy (DOE), Office of
809 Science, Office of Biological and Environmental Research. SPRUCE is collaborative research between Oak Ridge
810 National Laboratory and the USDA Forest Service Northern Research Station. Oak Ridge National Laboratory is
811 managed by UT-Battelle, LLC, for the U.S. DOE under contract DE-AC05-00OR22725. The USDA Forest Service
812 funds support the long-term research program at the Marcell Experimental Forest, chemistry analyses in Grand Rapids,
813 and the participation of Randy K. Kolka and Stephen D. Sebestyen in this research. This research was funded in part
814 by SeaGrant project number CON000000070744, project number 00085442 and supported the participation of Jessica
815 L. M. Gutknecht, Brandy M. Toner, and Edward A. Nater. Funding for this project was in-part provided by the
816 Minnesota Environment and Natural Resources Trust Fund as recommended by the Legislative-Citizen Commission
817 on Minnesota Resources (LCCMR) through award number ML 2017, CH 96, SEC 2, SUB 04I. A portion of the work
818 was conducted at the CLS, which is supported by the Canadian Foundation for Innovation, Natural Sciences and
819 Engineering Research Council of Canada, the University of Saskatchewan, the Government of Saskatchewan, Western
820 Economic Diversification Canada, the National Research Council Canada, and the Canadian Institutes of Health
821 Research.

822 **Competing Interests**

823 All authors declare they have no conflicts of interest.

824 **Author Contributions**

825 The study was designed and funded by grants prepared by Brandy Toner, Jessica Gutknecht, Randall Kolka, Stephen
826 Sebestyen, Natalie Griffiths, and Edward Nater. Sample collection was performed by Keith Oleheiser. Sample
827 analysis was performed by Caroline Pierce, Sona Psarska, Brandy Toner and Keith Oleheiser. Brandy Toner

828 developed the sulfur XANES method and workflow. Data analysis was performed by Caroline Pierce, Natalie
829 Griffiths, Jessica Gutknecht, and Brandy Toner. The manuscript was written by Caroline Pierce. All authors
830 commented on previous versions of the manuscript. All authors read and approved the final manuscript.

Supplementary Files

This is a list of supplementary files associated with this preprint. Click to download.

- 230410THgSPRUCEsupplementalver8cleancopy.docx